Contents lists available at ScienceDirect

Marine Pollution Bulletin

journal homepage: www.elsevier.com/locate/marpolbul

Relationship of photosynthetic carbon fixation with environmental changes in the Jiulong River estuary of the South China Sea, with special reference to the effects of solar UV radiation

Gang Li [a,b], Kunshan Gao [a,*], Dongxing Yuan [a], Ying Zheng [a], Guiyuan Yang [a]

[a] State Key Laboratory of Marine Environmental Science, Xiamen University, Xiamen, Fujian 361005, China
[b] Key Laboratory of Marine Bio-resources Sustainable Utilization, South China Sea Institute of Oceanology, CAS, Guangzhou, Guangdong 510301, China

ARTICLE INFO

ABSTRACT

Phytoplankton cells in estuary waters usually experience drastic changes in chemical and physical environments due to mixing of fresh and seawaters. In order to see their photosynthetic performance in such dynamic waters, we measured the photosynthetic carbon fixation by natural phytoplankton assemblages in the Jiulong River estuary of the South China Sea during April 24–26 and July 24–26 of 2008, and investigated its relationship with environmental changes in the presence or the absence of UV radiation. Phytoplankton biomass (Chl a) decreased sharply from the river-mouth to seawards (17.3–2.1 µg L^{-1}), with the dominant species changed from chlorophytes to diatoms. The photosynthetic rate based on Chl a at noon time under PAR-alone increased from 1.9 µg C (µg Chl a)$^{-1}$ L^{-1} in low salinity zone (SSS < 10) to 12.4 µg C (µg Chl a)$^{-1}$ L^{-1} in turbidity front (SSS within 10–20), and then decreased to 2.1 µg C (µg Chl a)$^{-1}$ L^{-1} in mixohaline zone (SSS > 20); accordingly, the carbon fixation per volume of seawater increased from 12.8 to 149 µg C L^{-1} h^{-1}, and decreased to 14.3 µg C L^{-1} h^{-1}. Solar UVR caused the inhibition of carbon fixation in surface water of all the investigated zones, by 39% in turbidity area and 7–10% in freshwater or mixohaline zones. In the turbidity zone, higher availability of CO_2 could have enhanced the photosynthetic performance; while osmotic stress might be responsible for the higher sensitivity of phytoplankton assemblages to solar UV radiation.

© 2011 Elsevier Ltd. All rights reserved.

1. Introduction

Estuarine ecosystems are susceptible to anthropogenic impacts because of the hydrodynamics associated with mixing of fresh and sea water and near-shore human activities (Kimmerer, 2002; Zhai et al., 2005). River-derived inputs of nutrients are known to stimulate growth of phytoplankton (Pennock and Sharp, 1986; Dai et al., 2008) and increase production of benthic invertebrates (Wilber, 1992) or fishes (Jassby et al., 1995). On the other hand, the inputs can also lead to light-limitation, osmotic stress and washout (Deegan, 1990; Colern, 1999; Gameiro et al., 2007). In some cases, the negative and positive effects are neutralized, giving rise to insignificant effects (Rose and Summers, 1992). Chemical (e.g., salinity, nutrients, pH, O_2 and pCO_2) and physical (e.g., turbidity and mixing) changes are known to influence the estuarine phytoplankton communities (Licursi et al., 2006; Gameiro et al., 2007). Primary production in estuary ecosystems thus varies greatly, ranging from 30 to 6500 mg C m^2 d^{-1} in Changjiang (Yangtze) River estuary (Yang et al., 2006) and from 2 to 4840 mg C m^2 d^{-1} in

Neuse River estuary (Boyer et al., 1993). Obviously, the physic-chemical environmental changes regulate the physiology of phytoplankton cells and the primary production in the estuaries.

Phytoplankton cells depend on solar PAR for photosynthesis; at the same time, they are often exposed to UV radiation (UVR, 280–400 nm) that can penetrate up to 60 m in the oceans (Smith and Baker, 1979). UVR damages DNA (Gao et al., 2008), destructs PSII (Lao and Glazer, 1996), bleaches pigments (Worrest et al., 1978), increases membrane permeability (Sobrino et al., 2004), reduces nitrate or phosphorus uptake (Sobrino et al., 2004) and ultimately decreases the primary production (Gao et al., 2007a; Li et al., 2009). It can also alter the species composition (Marcoval et al., 2008) and influence the food chain (Helbling and Zagarese, 2003). On the other hand however, moderate levels of longer UV wavelengths (mostly UV-A) can result in positive effects, such as enhancement of photosynthetic carbon fixation by the coastal phytoplankton assemblages (Gao et al., 2007a,b; Li et al., 2011), photorepairing of the UVB-damaged DNA (Malloy et al., 1997) and stimulation of the synthesis of mycosporine-like amino acids (MAAs) (Marcoval et al., 2008) that play protective roles against UVR. In the estuary waters, phytoplankton cells suffer from drastic changes in the chemical environment, therefore, their sensitivity to solar UVR may be influenced by the environmental changes.

---

* Corresponding author. Tel./fax: +86 592 2187963.
  E-mail address: ksgao@xmu.edu.cn (K. Gao).

Jiulong River estuary is situated at the northern part of the South China Sea that has been increasingly polluted during the last decades. The rapid development of this district has brought about environmental pressures on this estuary ecosystem (Hong et al., 1995; Zhou et al., 2000; Maskaoui et al., 2002). Therefore, many studies have so far been carried out to characterize its hydrodynamics, physical and chemical environments as well as biological features (Hong et al., 1995; Zhang et al., 1999; Huang et al., 2001; Yuan et al., 2001; Maskaoui et al., 2002). However, little has been documented on the *in situ* photophysiological behavior of phytoplankton cells and its relationship to the environmental changes in this estuary. In this paper, we showed the relationship of photosynthetic carbon fixation with environmental gradients and the responses of phytoplankton assemblages to solar UV radiation.

2. Materials and methods

2.1. Study area/sampling protocol

Jiulong River estuary in the northern South China Sea (Fig. 1) is shallow (3–16 m in depth) with a watershed area of about 130 km^2, and strongly influenced by the tidal changes. Tides in this estuary are predominately semi-diurnal with the maximum tidal range of 4.5 m, varying from 1.0 m during neap tides to 5.5 m during spring tides, and there is little seasonal variation. Mean amount of the freshwater outflow from the river reached 1.17×10^{10} m^3 per year, ranging between 8.7×10^9 m^3 per year in rainy season (i.e., from April to September) and 3.0×10^9 m^3 per year in dry season (i.e., from October to next March). Since the drastic environmental changes were often controlled by the land-derived runoffs in the estuary, the experiments were thus designed in rainy season (e.g., April and July) to determine the phytoplankton photosynthetic responses to such environmental changes.

During the two cruises (April 24–26 and July 24–26) of 2008, the investigations were performed in the morning periods (8:00–10:00, high tide) and successively preceded to riverward at the 1st day, seaward at the 2nd day and from the middle to riverward, then back to seaward at the 3rd day. Surface seawater (at about 10 cm depth) was sampled at each station (Fig. 1) with an acid-cleaned (1 N HCl) polycarbonate container (5 L) and used immediately (within 5 min) for the experiments as well as related-analyses described below.

2.2. Measurements of temperature, salinity, DO, nutrients, DIC and light

At each station, profiles of salinity, temperature and dissolved oxygen (DO) were obtained prior to the water sampling with a
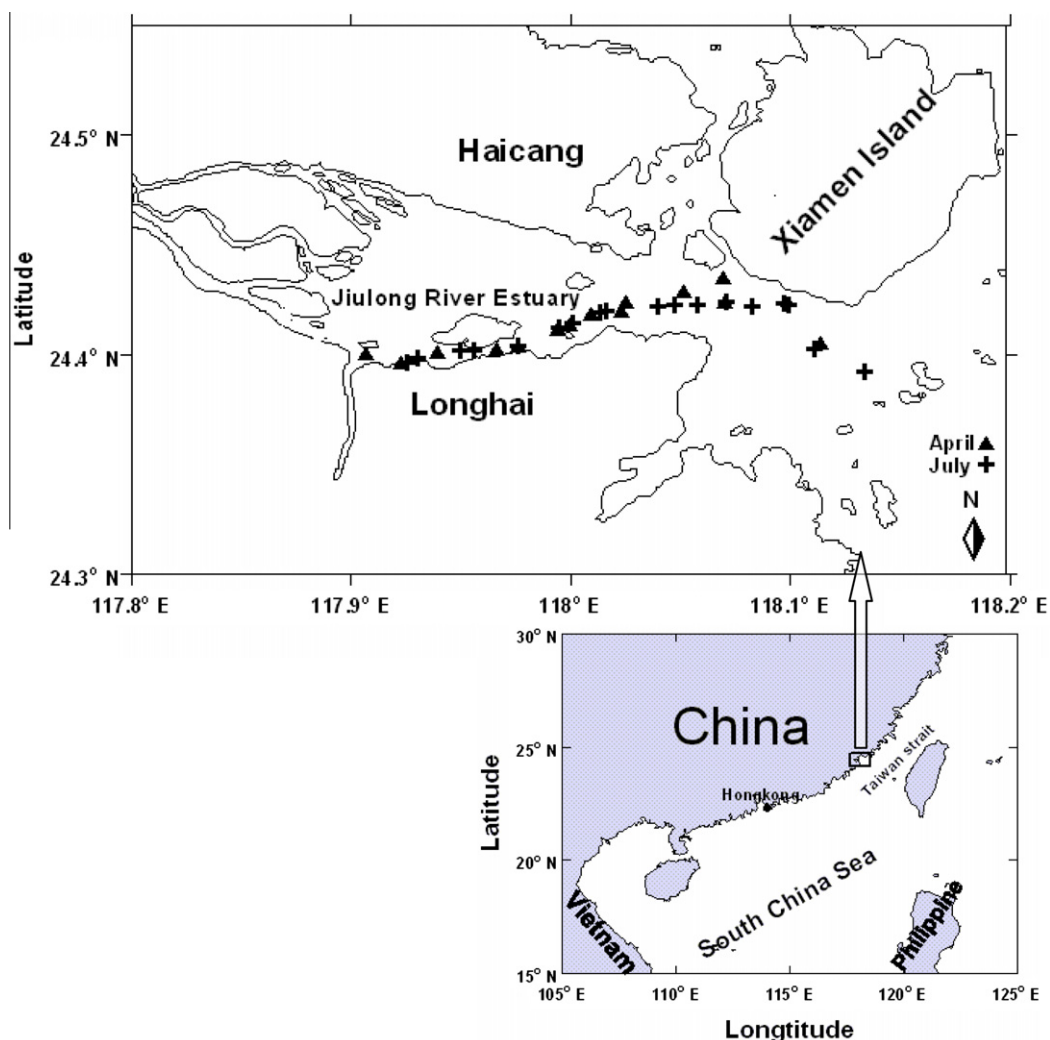

Fig. 1. Location of Jiulong River estuary and the sampling sites during the cruises (April 24–26 and July 24–26, 2008).

SONDE (YSI 600QS, Yellow Spring Instruments, USA). For determination of nutrients (i.e., NH_4^+, NO_3^-, NO_2^-, PO_4^{3-} and SiO_3^{2-}), 800 ml surface seawater was collected at each station, and stored at 4 °C until the analyses were performed within 6 h in the laboratory. Nitrate or, nitrite and ammonium were determined colorimetrically following the procedures of Wood et al. (1967) and Pai et al. (2001), respectively. Manual analyses of phosphate and silicate were based on the methods by Murphy and Rilly (1962) and Armstrong et al. (1967). The dissolved inorganic carbon (DIC) was measured with a DIC analyzer (AS-C3, Apollo SciTech, USA), following the description by Cai et al. (2004).

Underwater light profiles were obtained using a diving broadband filter radiometer (ELDONET, Real Time Computers Inc., Germany) that records every second the light irradiance in three wavebands: UV-B (280–315 nm), UV-A (315–400 nm) and PAR (400–700 nm), as well as the temperature and depth. At the same time, a terrestrial radiometer (ELDONET, Real Time Computers Inc., Germany), installed on the roof of a building (24° 26′ N, 118° 05′ E, within 1.5 km distance from the estuary area) of Xiamen University, was used to continuously measure the incident solar irradiances. Both the devices were calibrated regularly with the support of the maker against a double monochromator spectroradiometer (HR4000, Oceanic Optics Inc., USA) and a certified calibration lamp (DH 2000, Oceanic Optics Inc., USA).

2.3. Measurements of photosynthetic carbon fixation

To determine the carbon fixation of phytoplankton assemblages, pre-filtered (pore-size, 180 μm) water sample was dispensed into 50 ml quartz tubes and inoculated with 50 μl–2.5 μCi (92.5 KBq) $NaH^{14}CO_3$ solution (ICN Radiochemicals, USA). At each station, triplicate tubes were either exposed to full solar radiation (PAB, 280–700 nm; uncovered quartz tubes) or PAR-alone [P, 400–700 nm; quartz tubes wrapped with Ultraphan 395 foil (UV Opak, Digefra, Munich, Germany)]; while the dark control was run in duplicate (wrapped in aluminum foil). The transmission spectra of the tubes and cut-off foil were published elsewhere (Li et al., 2010). The tubes containing the sample were placed beneath the surface of a water bath through which the surface seawater was continuously pumped for the control of temperature to the same levels of the SST (22–24 °C in April and 29–31 °C in July). The incubation lasted for 3–4 h centered on local noon. After the incubation, the sample was filtered onto a Whatman GF/F glass fiber filter (25 mm), that was then placed into a 20 ml scintillation vial, exposed to HCl fumes overnight and dried (55 °C, 6 h) to expel the non-fixed ^{14}C. Consequently, 3 ml scintillation cocktail (Perkin–Elmer®) was added to each vial and the radioactivity was counted with a liquid scintillation counter (LS 6500, Beckman Coulter, USA). The rate of photosynthetic carbon fixation was calculated according to Holm-Hansen and Helbling (1995). A total of 32 incubations were carried out during the two cruises.

2.4. Chlorophyll a and species analyses

At each station and at the beginning of each experiment, 300–500 ml of surface seawater was filtered on a Whatman GF/F glass fiber filter (25 mm) that was immediately frozen and stored in −20 °C for extraction and measurement of chlorophyll a (Chl a) concentration. The content of Chl a was determined spectrophotometrically using a scanning spectrophotometer (DU800, Beckman Coulter, USA) according to Porra (2002).

For species analysis, the surface seawater was fixed with buffered formalin (final concentration of 0.4%). The quantitative analyses and examination of phytoplankton cells were carried out with an inverted microscope (TS100 Nikon, Japan) after settling 10 ml of

samples in Utermöhl Chamber (Hydro-Bios Kiel, Germany) for 24 h (Villafañe and Reid, 1995).

2.5. Statistics

One-way ANOVA and paired t-test were used to determine significant differences ($p < 0.05$) among the estimated parameters, the correlation between variables was established using a Kendall's τ test.

3. Results

Within 21 km downstream along the estuary, surface seawater salinity (SSS) increased from 3.68 to 27.1 in April and from 0.80 to 28.3 in July (Fig. 2A), while the temperature (SST) decreased correspondingly from 22.6 to 20.5 °C and from 30.6 to 28.2 °C (Fig. 2B). The dissolved oxygen (DO) increased from 5.47 to 7.93 mg L^{-1} in April and from 3.57 to 7.58 mg L^{-1} in July (Fig. 2C). The SST was lower and the DO was higher in April, compared to that in July; whereas the higher values of SSS in April than that of July were merely observed at stations within 12 km (SSS < 18) from the river-mouth, and no significant difference ($p > 0.05$) was detected at the stations beyond (Fig. 2). With increasing distance from the river-mouth to seawards, depths of 1% penetrated PAR (UV-A, UV-B) increased from 0.47 to 5.01 m (0.25–2.84, 0.22–1.66 m) in April and from 0.29 to 4.42 m (0.15–2.79, 0.10–1.50 m) in July (Fig. 3), with the attenuation coefficients of PAR (UV-A, UV-B) decreasing from 9.59 to 0.92 m^{-1} (18.4–1.62, 20.9–2.77 m^{-1}) and from 15.8 to 1.04 m^{-1} (30.7–1.65, 46.1–3.07 m^{-1}), respectively. The euphotic zone was deeper in April than that of July, especially at upstream of the estuary (Fig. 3A), reflecting the reduced transparency in estuary due to the freshwater outflows. The measured surface PAR levels
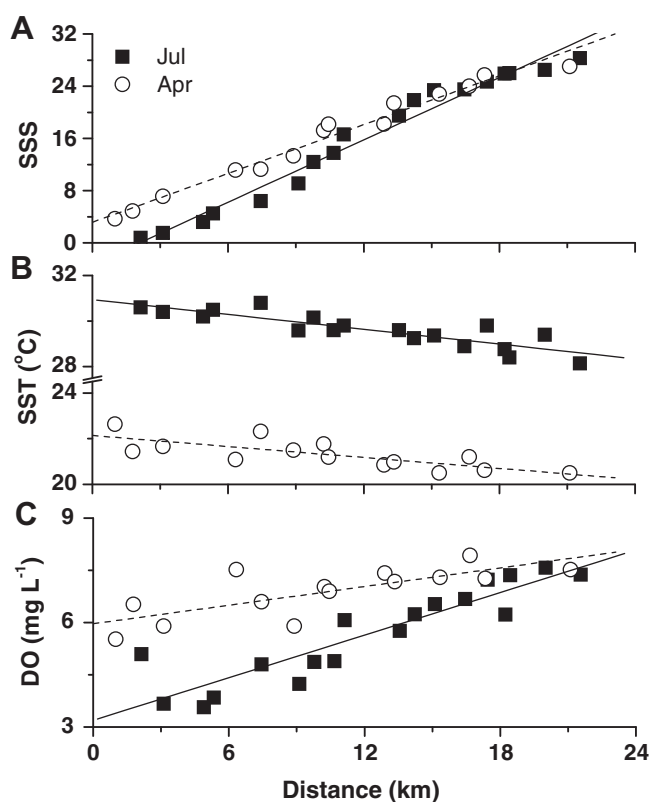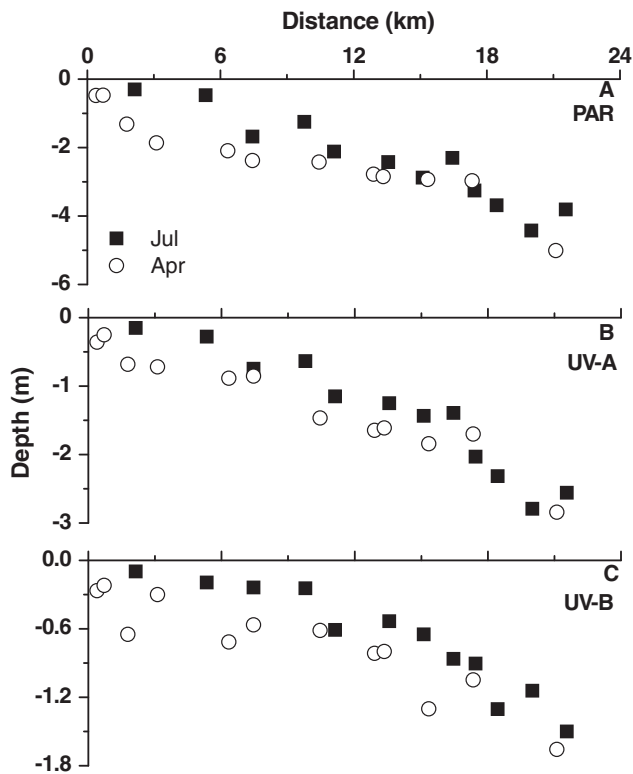

Fig. 2. Spatial variations of surface seawater salinity (A, SSS), temperature (B, SST, °C) and dissolved oxygen (C, DO, mg L^{-1}) from the river-mouth to seawards along Jiulong River estuary.

Fig. 3. Spatial variations of underwater light (UV)-penetrated depth (m, at 1% of surface level): PAR (A, 400–700 nm), UV-A (B, 315–400 nm) or UV-B (C, 280–315 nm).

Fig. 4. Spatial variations of surface nutrients concentration (μM) from the river-mouth to seawards: nitrite (A, NO_2^-), nitrate (B, NO_3^-), ammonium (C, NH_4^+); phosphate (D, PO_4^{3-}) and silicate (E, SiO_3^{2-}).

during the experimental cruises were 273 ± 77 and $346 \pm 32\ W\,m^{-2}$; while UV-A (UV-B) reached $40.6 \pm 11\ W\,m^{-2}$ ($1.96 \pm 0.59\ W\,m^{-2}$) and $46.8 \pm 4.5\ W\,m^{-2}$ ($2.17 \pm 0.17\ W\,m^{-2}$) in April and July, respectively.

Concentrations of NO_3^-, NO_2^-, NH_4^+, PO_4^{3-} and SiO_3^{2-} decreased sharply from the river-mouth (Fig. 4). The nitrate, representing 80% of the dissolved inorganic nitrogen, decreased by 3.6% per km from 183 to 44.0 μM (Fig. 4A), while that of nitrite and ammonium declined by 3.9% (29.8–5.10 μM) and 4.1% per km (42.1–5.71 μM) (Fig. 4B and C). Drastic reduction of phosphorus and silicate concentrations to seawards was found as well, with the values ranged from 1.73 to 0.81 μM and from 252 to 72.9 μM (Fig. 4D and E). The NO_3^-, NO_2^- and NH_4^+ concentrations were slight higher in April than that of July, especially at the river-mouth (Fig. 4A–C); while no significant difference ($p > 0.05$) in PO_4^{3-} was observed between the two cruises (Fig. 4D). Finally, the lower silicate concentration in April than July was merely detected at the stations within 12 km from the river mouth, but no significant difference ($p > 0.05$) presented at the rest stations investigated (Fig. 4E).

Phytoplankton biomass (Chl a) in surface seawater showed a strong spatial variation from the river-mouth to seawards, with Chl a concentration decreasing from 9.92 to 1.62 μg L^{-1} in April and from 17.3 to 4.3 μg L^{-1} in July (Fig. 5A). As the SSS increased downstream, the dominant species of phytoplankton groups changed from chlorophytes (e.g., *Scenedesmus* spp.) to diatoms (e.g., *Skeletonema costatum*, *Chaetoceros* sp., *Coscinodiscus* spp. and *Thalassionema* sp.). In the turbidity front (SSS within 10–20), the diatoms were abundant, though green algal species were also found. Photosynthetic carbon fixation capacity per volume of seawater, which was determined during noon period under PAR alone, increased from $12.8\ \mu g\,C\,L^{-1}\,h^{-1}$ in river-mouth to $67.6\ \mu g\,C\,L^{-1}\,h^{-1}$ in turbidity front, and then decreased to
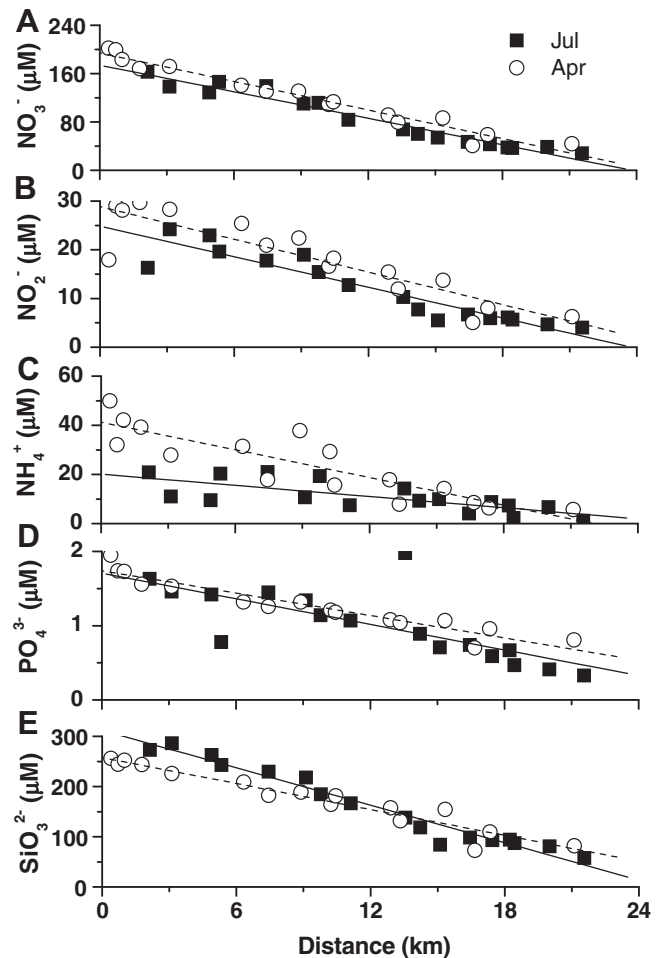
$11.4\ \mu g\,C\,L^{-1}\,h^{-1}$ in adjacent water to open-sea (Fig. 5B); correspondingly, the assimilation number (ASN) increased from 1.59 to 14.4 μg C (μg Chl a)$^{-1}$ h^{-1}, and then decreased to 6.83 μg C (μg Chl a)$^{-1}$ h^{-1} (Fig. 5C). Similar trend was found in the cruise of July, with higher values than that in April (Fig. 5B and C). The maximal carbon fixation capacity and ASN were about 55% and 20% higher in July than in April, respectively.

When the photosynthetic carbon fixation rate was plotted against the gradients of nutrients (i.e., NO_2^-, NO_3^-, NH_4^+, PO_4^{3-} and SiO_3^{2-}), positive correlations were highly significant ($p < 0.05$) in April cruise at the adjacent-open-sea (SSS > 18, Table 1); while at the river-mouth (SSS < 18), no such significant relationships ($p > 0.05$) were detected in most of the cases (Table 1), which indicated that the photosynthetic capacity was to some extent conditioned by the nutrients-level in high-saline-water zones. On the other hand, there was a positive relationship between photosynthetic rate and DIC concentration at river-mouth area, but no such phenomenon was observed at adjacent open-sea waters (Fig. 6), suggesting the DIC density might control the photosynthetic rate of phytoplankton in freshwater zones. Similar relationships occurred in the cruise of July. In particular the presence of solar UVR significantly reduced the photosynthetic carbon fixation in all the investigated zones, especially in turbidity zone with the inhibition being up to 39%. UVR inhibited the photosynthetic rate by 7–10% in the freshwater or mixohaline zones (Fig. 7, Table 1).

Fig. 5. Biological characteristics in surface seawater for the two cruises along the estuary: (A) phytoplankton biomass (Chl *a*, µg L^{-1}), (B) carbon fixation capacity (µg C L^{-1} h^{-1}) and (C) assimilation number (µg C (µg Chl *a*)$^{-1}$ h^{-1}) of phytoplankton assemblages exposed to PAR-alone (400–700 nm). Vertical bars represent the standard deviations (*n* = 3).

4. Discussion

Estuarine ecosystems are sensitive to a variety of environmental factors that often changed due to the land-derived runoff or tide-induced water exchange. Enriched nutrients in Pearl River estuary stimulated phytoplankton growth (Yin et al., 2001; Dai et al., 2008); while reduced light availability and osmotic stress influenced the primary production in Delaware estuary (Pennock and Sharp, 1986) and Tagus estuary (Gameiro et al., 2007). In Jiulong River estuary, phytoplankton biomass (Chl *a*) decreased by 0.41 and 0.59 µg L^{-1} per km from river-mouth to seawards in the cruises of April and July, respectively; however, the photosynthetic C-fixation rate increased by 1.48 and 5.46 µg L^{-1} h^{-1} per km from river-mouth to half-fresh water, then decreased by 4.64 and 5.06 µg L^{-1} h^{-1} per km to adjacent open-sea. Maximum

Fig. 6. Phytoplankton photosynthetic rate (µg C (µg Chl *a*)$^{-1}$ h^{-1}) as a function of dissolved inorganic carbon (DIC, mmol L^{-1}) or salinity. Vertical bars represent the standard deviations (*n* = 3).

Fig. 7. Spatial variability of photosynthetic carbon fixation ratios of PAB (280–700 nm) to P (400–700 nm) treatments from river-mouth to seawards. Vertical bars represent the standard deviations (*n* = 3).

photosynthetic capacity based on both Chl *a* and volume of surface seawater was found at half-fresh water, where the phytoplankton cells were more sensitive to solar UV radiation.

Table 1
R and *p* values of the photosynthetic carbon fixation (µg C L^{-1} h^{-1}) being plotted against the gradients of nutrients (i.e., NO_2^-, NO_3^-, NH_4^+, PO_4^{3-} and SiO_3^{2-}) in µM in the river-mouth (SSS < 18) and adjacent-open-sea (SSS > 18) waters. The stars (*) represent the significant difference.

Nutrients (µM)	April				July			
	$R_{(SSS<18)}$	p	$R_{(SSS>18)}$	p	$R_{(SSS<18)}$	p	$R_{(SSS>18)}$	p
NO_2^-	0.161	0.678	0.854	0.015*	−0.177	0.704	0.581	0.048*
NO_3^-	−0.378	0.316	0.815	0.025*	−0.777	0.040*	0.672	0.033*
NH_4^+	−0.784	0.013*	0.840	0.018*	−0.258	0.576	0.824	0.003*
PO_4^{3-}	−0.522	0.150	0.762	0.046*	0.102	0.827	0.563	0.050*
SiO_3^{2-}	−0.487	0.184	0.810	0.027*	−0.657	0.109	0.641	0.046*

Dramatic environmental gradients often prevail the Jiulong River estuary, such as temperature and salinity (Fig. 2), light penetration (Fig. 3) and concentrations of nutrients (Fig. 4), which is consistent with what has been previously reported (Zhang et al., 1999; Zhou et al., 2000). Freshwater outflow was one of the controlling factors for the decreased salinity and the increased levels of nutrients (Kimmerer, 2002); while tide-induced turbidity and nutrients-powered blooms of phytoplankton could be the main causes for the decline of light penetration (Colern, 1999). In the Pearl River estuary, eutrophication-induced algal blooms usually draw down pCO_2 in the surface water due to enhanced photosynthesis (Dai et al., 2008), though pCO_2 increases occasionally due to active aerobic respiration (Zhai et al., 2005). Changes in the CO_2 and light availability due to the chemical, physical and biological dynamics in the estuary ecosystem modulate the photosynthetic carbon fixation by phytoplankton cells over short- as well as over long-term time scales, which is reflected in the present study (Fig. 7) or in others (Boyer et al., 1993; Kimmerer, 2002).

Similar to the trend of nutrients-level (Fig. 4), phytoplankton biomass (Chl *a*) drastically decreased seawards (Fig. 5A); however, the photosynthetic capacity increased from river-mouth to turbidity fronts, but then decreased to open-sea area (Fig. 5B and C). Light penetration, mainly regulated by riverine inputs and tidal turbidity, is known to be an important factor influencing the phytoplankton blooms in the estuaries (Pennock and Sharp, 1986; Colern, 1999). In Jiulong River estuary, the euphotic zone was less than 2 m (Fig. 3) and Chl *a* concentration was high at river mouth (Fig. 5A), but photosynthetic carbon fixation rate was low (Fig. 5B). The freshwater-derived phytoplankton cells must have been stressed upon the exposure to seawater and thus resulted in low photosynthetic activity. The discrepancy between phytoplankton biomass and photosynthetic carbon fixation capacity at the river-mouth (Fig. 5A and B) could also be attributed to the low DIC contents (Fig. 6) or/and reduced availability of solar energy (Fig. 3). Low DIC concentration often limits growth of phytoplankton cells in freshwater (Hein, 1997), while reduced light availability in estuary could also limit the growth of the cells (Colern, 1999). On the other hand, lowered pH caused by effluent freshwater could lead to higher partial pressure of CO_2 (Zhai et al., 2005) and thus enhance photosynthesis of some phytoplankton species that shows limited photosynthesis at ambient CO_2 level (Fig. 6) (Hein, 1997).

Solar UVR gave rise to a significant reduction in photosynthetic carbon fixation at all the stations investigated (Fig. 7). The UV-induced inhibition of photosynthetic rate was higher in half-freshwater (SSS, 18), compared to that in fresh- or saline-water (Fig. 7). Osmotic stress could interact with UV to reduce the photosynthetic rate of both freshwater and marine phytoplankton species that are mixed via affecting their defensive or repairing pathways (Helbling and Zagarese, 2003), leading to enhanced photosynthetic inhibition caused by UVR (Fig. 7). UVR in combination with salt-stressed could also cause additional oxidative stressors that reduced the photosynthetic efficiency and decreased the cell-division rates of phytoplankton (Rijstenbil, 2003). On the other hand, availability of nutrients such as nitrogen (N) or phosphorus (P) could potentially affect the susceptibility of phytoplankton to UVR (Litchman et al., 2002; Shelly et al., 2005). In the Jiulong estuary, P deficiency was reported based on Redfield N:P molar ratios (i.e., 69.1–147 in April and 46.7–128 in July) (Huang et al., 2001). The P starvation may promote the photoinhibition caused by UVR (Shelly et al., 2005), leading to more reduction of carbon fixation (Fig. 7).

Acknowledgments

References

Armstrong, F.A.J., Stearns, C.R., Strickland, J.D.H., 1967. The measurement of upwelling and subsequent biological processes by means of the technician auto-analyzer and associated equipment. Deep-Sea Res. 14, 381–389.

Boyer, J.N., Christian, R.R., Stanley, D.W., 1993. Patterns of phytoplankton primary productivity in the Neuse River estuary, North Carolina, USA. Mar. Ecol. Prog. Ser. 97, 287–297.

Cai, W., Dai, M., Wang, Y., Zhai, W., Huang, T., Chen, S., Zhang, F., Chen, Z., Wang, Z., 2004. The biogeochemistry of inorganic carbon and nutrients in the Pearl River estuary and the adjacent Northern South China Sea. Cont. Shelf Res. 24, 1301–1319.

Colern, J.E., 1999. The relative importance of light and nutrient limitation of phytoplankton growth: a simple index of coastal ecosystem sensitivity to nutrient enrichment. Aquat. Ecol. 33, 3–16.

Dai, M., Zhai, W., Cai, W., Callahan, J., Huang, B., Shang, S., Huang, T., Li, X., Lu, Z., Chen, W., Chen, Z., 2008. Effects of an estuarine plume-associated bloom on the carbonate system in the lower reaches of the Pearl River estuary and the coastal zone of the northern South China Sea. Cont. Shelf Res. 28, 1416–1423.

Deegan, L.A., 1990. Effects of estuarine environmental conditions on population dynamics of young-of-the-year gulf menhaden. Mar. Ecol. Prog. Ser. 68, 195–205.

Gameiro, C., Cartaxana, P., Brotas, V., 2007. Environmental drivers of phytoplankton distribution and composition in Tagus Estuary, Portugal. Estuar. Coast. Shelf Sci. 75, 21–34.

Gao, K., Li, G., Helbling, E.W., Villafañe, V.E., 2007a. Variability of UVR effects on photosynthesis of summer phytoplankton assemblages from a tropical coastal area of the South China Sea. Photochem. Photobiol. 83, 802–809.

Gao, K., Wu, Y., Li, G., Wu, H., Villafañe, V.E., Helbling, E.W., 2007b. Solar UV-radiation drives CO_2-fixation in marine phytoplankton: a double-edged sword. Plant Physiol. 144, 54–59.

Gao, K., Li, P., Watanabe, T., Helbling, E.W., 2008. Combined effects of ultraviolet radiation and temperature on morphology, photosynthesis, and DNA of *Arthrospira* (spirulina) *platensis* (Cyanophyta). J. Phycol. 44, 777–786.

Hein, M., 1997. Inorganic carbon limitation of photosynthesis in lake phytoplankton. Freshwater Biol. 37, 545–552.

Helbling, E.W., Zagarese, H.E., 2003. UV Effects in Aquatic Organisms and Ecosystems. The Royal Society of Chemistry, Cambridge, UK.

Holm-Hansen, O., Helbling, E.W., 1995. Técnicas para la medición de la productividad primaria en el fitoplancton. In: Alveal, K., Ferrario, M.E., Oliveira, E.C., Sar, E. (Eds.), Manual de Métodos Ficológicos. Universidad de Concepción, Concepción, Chile, pp. 329–350.

Hong, H., Xu, L., Zhang, L., Chen, J.C., Wong, Y.S., Wan, T.S.M., 1995. Environmental fate and chemistry of organic pollutants in the sediments of Xiamen and Victoria Harbors. Mar. Pollut. Bull. 31, 229–236.

Huang, B., Hong, H., Xue, X., 2001. Distribution and controlling factors of alkaline phosphatase activity in western Xiamen waters. Acta Oceanol. Sin. 22, 61–67.

Jassby, A.D., Kimmerer, W.J., Monismith, S.G., Armor, C., Cloern, J.E., Powell, T.M., Schubel, J.R., Vendlinski, T.J., 1995. Isohaline position as habitat indicator for estuarine populations. Ecol. Appl. 5, 272–289.

Kimmerer, W.J., 2002. Effects of freshwater flow on abundance of estuarine organisms: physical effects or trophic linkages? Mar. Ecol. Prog. Ser. 243, 39–55.

Lao, K., Glazer, A.N., 1996. Ultraviolet-B photodestruction of a light-harvesting complex. Proc. Natl. Acad. Sci. USA 93, 5258–5263.

Li, G., Wu, Y., Gao, K., 2009. Effects of typhoon KAEMI on coastal phytoplankton assemblages in the South China Sea, with special reference to the effects of solar UV radiation. J. Geophys. Res. G04029. doi:10.1029/2008JG000896.

Li, G., Gao, K., Gao, G., 2011. Differential impacts of solar UV radiation on photosynthetic carbon fixation from the coastal to offshore surface waters in the South China Sea. Photochem. Photobiol. 87, 329–334.

Licursi, M., Sierra, M.V., Gómez, N., 2006. Diatom assemblages from a turbid coastal plain estuary: Rio de la Plata (South America). J. Mar. Syst. 62, 35–45.

Litchman, E., Neale, P.J., Banaszak, A.T., 2002. Increased sensitivity to ultraviolet radiation in nitrogen-limited dinoflagellates: photoprotection and repair. Limnol. Oceanogr. 47, 86–94.

Malloy, K.D., Holman, M.A., Mitchell, D., Detrich, H.W., 1997. Solar UV-B-induced DNA damage and photoenzymatic DNA repair in Antarctic zooplankton. Proc. Natl. Acad. Sci. USA 94, 1258–1263.

Marcoval, M.A., Villafañe, V.E., Helbling, E.W., 2008. Combined effects of solar ultraviolet radiation and nutrients addition on growth, biomass and taxonomic composition of coastal marine phytoplankton communities of Patagonia. J. Photochem. Photobiol. B 91, 157–166.

Maskaoui, K., Zhou, J., Hong, H., Zhang, Z., 2002. Contamination by polycyclic aromatic hydrocarbons in the Jiulong River estuary and Western Xiamen Sea, China. Environ. Pollut. 118, 109–122.

Murphy, J., Rilly, J.P., 1962. A modified single solution method for the determination of phosphate in natural waters. Anal. Chim. Acta 27, 31–36.

Pai, S.C., Tsau, Y.J., Yang, T.I., 2001. PH and buffering capacity problems involved in the determination of ammonia in saline water using the indophenol blue spectrophotometric method. Anal. Chim. Acta 434, 209–216.

Pennock, J.R., Sharp, J.H., 1986. Phytoplankton production in the Delaware Estuary: temporal and spatial variability. Mar. Ecol. Prog. Ser. 34, 143–155.

Porra, R.J., 2002. The chequered history of the development and use of simultaneous equations for the accurate determination of chlorophylls a and b. Photosynth. Res. 73, 149–156.

Rijstenbil, J.W., 2003. Effects of UVB radiation and salt stress on growth, pigments and antioxidative defense of the marine diatom *Cylindrotheca closterium*. Mar. Ecol. Prog. Ser. 254, 37–48.

Rose, K.A., Summers, J.K., 1992. Relationships among long-term fisheries abundance, hydrographic variables, and gross pollution indicators in northeastern US estuaries. Fish Oceanogr. 1, 281–293.

Shelly, K., Roberts, S., Heraud, P., Beardall, J., 2005. Interactions between UV-B exposure and phosphorus nutrition. I. Effects on growth, phosphate uptake, and chlorophyll fluorescence. J. Phycol. 41, 1204–1211.

Smith, R.C., Baker, K.S., 1979. Penetration of UV-B and biologically effective dose-rates in natural waters. Photochem. Photobiol. 29, 311–323.

Sobrino, C., Montero, O., Lubian, L.M., 2004. UV-B radiation increases cell permeability and damages nitrogen incorporation mechanisms in *Nannochloropsis gaditana*. Aquat. Sci. 66, 421–429.

Villafañe, V.E., Reid, F.M.H., 1995. Métodos de microscopía para la cuantificación del fitoplancton. In: Alveal, K., Ferrario, M.E., Oliveira, E.C., Sar, E. (Eds.), Manual de Métodos Ficológicos. Universidad de Concepción, Concepción, Chile, pp. 169–185.

Wilber, D.H., 1992. Associations between freshwater inflows and oyster productivity in Apalachicola Bay, Florida. Estuar. Coast. Shelf Sci. 35, 179–190.

Wood, E.D., Armstrong, F.A.J., Richards, F.A., 1967. Determination of nitrate in seawater by cadmium–copper reduction to nitrite. J. Mar. Biol. Assoc. UK 47, 23–31.

Worrest, R.C., Van Dyke, H., Thomson, B.E., 1978. Impact of enhanced simulated solar ultraviolet radiation upon a marine community. Photochem. Photobiol. 27, 471–478.

Yang, D., Wang, F., Gao, Z., Chen, Y., Xie, L., 2006. An approach to the effect of physicochemical factors on primary production in the changjiang estuary (in Chinese with English abstract). Adv. Mar. Sci. 24, 97–107.

Yin, K., Qian, P.Y., Wu, M.C.S., Chen, J.C., Huang, L., Song, X., Jian, W., 2001. Shift from P to N limitation of phytoplankton growth across the Pearl River estuarine plume during summer. Mar. Ecol. Prog. Ser. 211, 17–28.

Yuan, D., Yang, D., Wade, T.L., Qian, Y., 2001. Status of persistent organic pollutants in the sediment from several estuaries in China. Environ. Pollut. 114, 101–111.

Zhai, W., Dai, M., Cai, W.J., Wang, Y., Wang, Z., 2005. High partial pressure of CO_2 and its maintaining mechanism in a subtropical estuary: the Pearl River estuary, China. Mar. Chem. 93, 21–32.

Zhang, Y., Wang, W., Huang, Z., 1999. Salinity front and chemical behavior of nutrient in Jiulongjiang Estuary. Mar. Environ. Sci. 18, 1–7 (in Chinese with English abstract).

Zhou, J., Hong, H., Zhang, Z., Maskaoui, K., Chen, W., 2000. Multi-phase distribution of organic micropollutants in Xiamen Harbor, China. Water Res. 34, 2132–2150.